Energy Conversion
Circuit Laboratory

# Mitigation Method of the Shaft Voltage according to Parasitic Capacitance of the PMSM

Jun-kyu Park[1], Thusitha Wellawatta[1], Sung-Jin Choi[1], and Jin Hur[2]
[1]School of Electrical Engineering, University of Ulsan, Ulsan, South Korea
[2]Dept. of Electrical Engineering, Incheon National University, Incheon, South Korea
jinhur@inu.ac.kr

***Abstract*— In this study, we propose the mitigation method of a shaft voltage according to change in parasitic capacitances of a permanent magnet synchronous motor (PMSM). First, we designed the equivalent circuit taking into account all parasitic capacitances. Then, we deducted that rotor-to-winding and stator-to-rotor capacitances mainly affect the shaft voltage. The stator-to-rotor capacitance depends on the air-gap length, which directly affects output torque characteristics of the motor. In case of the rotor-to-winding capacitance, it depends on the distance from the rotor to winding, which have effects on torque ripple, but it doesn't affect average torque of the motor. Thus, rotor-to-winding capacitance is determined as a variable for mitigation of the shaft voltage. According to change in the rotor-to-winding capacitance, we obtained and compared the results of the shaft voltage, average torque, and torque ripple.**

***Keywords*—Brushless DC motor, bearing current, common-mode current, common-mode voltage, equivalent circuit, parasitic capacitance, shaft voltage.**

## I. Introduction

Permanent magnet synchronous motors (PMSMs) driven by a space vector pulse width modulation (SVPWM) inverter are widely used in lots of industrial fields due to their high power density, high torque, and free maintenance. In the drive system, however, they have the major cause of motor bearing failure due to fast switching of the SVPWM [1], [2]. Practically, all SVPWM inverters generate a common-mode voltage (CMV) relative to the ground, which creates a shaft voltage through parasitic capacitances of the motor. Specifically, the CMV causes the shaft voltage, and finally it provides bearing current due to capacitive coupling between stator, rotor, and winding [3]–[5].

In the motor drive system, shaft voltage can be classified into two types such as a shaft-to-stator frame voltage and end-to-end voltage, as shown in Fig. 1 [6], [7]. First, shaft-to-stator frame voltage is occurred by parasitic capacitance link with the rotor shaft and winding, and it creates a voltage drop with the ground. In addition, shaft-to-stator frame voltage can be detected by connecting the shaft and stator frame. Here, motor inverter is also grounded, thus it creates a close current path [8]. Second, end-to-end voltage is occurred by induced electromotive force (EMF) in the shaft. It does not cause a current flow through the ground. However, circulating current tries to flow through the stator frame via bearings, as shown in Fig. 1. In addition, end-to-end shaft voltage can be detected by connecting shaft the drive end and the non-drive end [6].

In this study, a mitigation method of the shaft voltage due to parasitic capacitances is proposed within a range that does not affect the average torque. Specifically, there are two kinds of parasitic capacitances, which are the main cause of the shaft voltage such as stator-to-rotor and rotor-to-winding capacitances. The stator-to-rotor capacitance highly affects the average torque because it depends on the air-gap length. On the other hand, rotor-to-winding capacitance scarcely affects the average torque because it depends on the distance between the rotor and winding. Thus, we analyzed average torque, torque ripple, and shaft voltage according to change in the rotor-to-winding capacitance in order to minimize the shaft voltage taking into account torque characteristics.

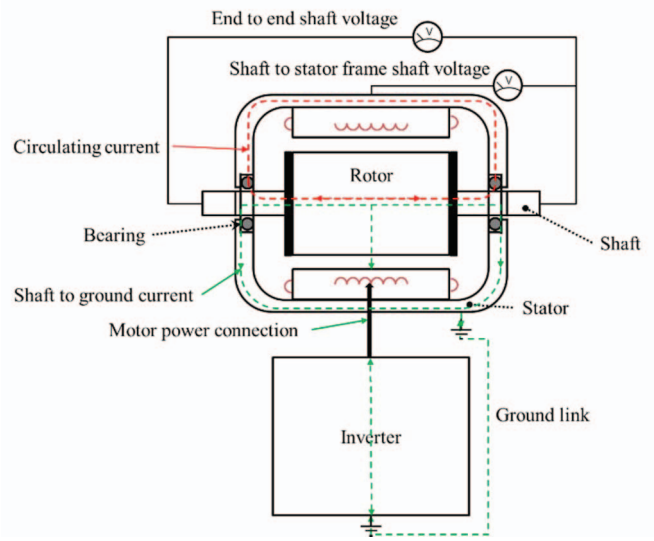


Fig. 1.System overview.

978-1-5090-0737-0/16/$31.00 ©2016 IEEE

## II. Equivalent Circuit by All Parasitic Capacitances

This section introduces the procedure to design an equivalent circuit using parasitic capacitance. First, all parasitic capacitances are determined taking into account the motor geometry, as shown in Fig. 2 (a). Table 1 denotes the definition of each capacitance. Next, parameters of the motor structure are demonstrated to calculate all parasitic capacitances according to the geometry of the motor, as shown in Fig. 2 (b). Table II shows the dimensions of the motor structure.

### A. All parasitic capacitances

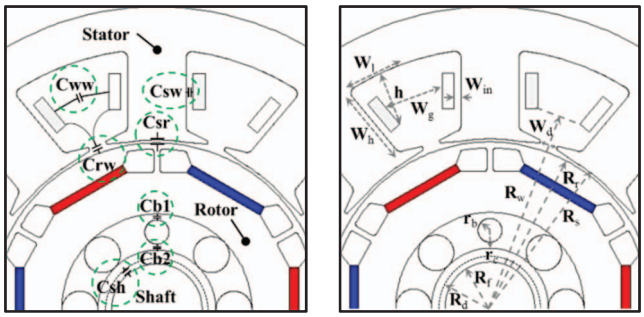


(a) (b)

Fig. 2. Configurations of capacitance dimensions in the motor. (a) Parasitic capacitances. (b) Parameters for motor structure.

TABLE I:
Definition of All Parasitic Capacitance

| Item | Appearance |
|---|---|
| Csw | Capacitance of stator-to-winding |
| Crw | Capacitance of rotor-to-winding |
| Csr | Capacitance of stator-to-rotor |
| Cww | Capacitance of winding-to-winding |
| Cbt | Capacitance of end bearings (Cb1=Cb2=2Cb) |
| Csh | Capacitance of shaft hall |

TABLE II:
Dimensions of Motor Structure

| Item | Appearance | Value | Units |
|---|---|---|---|
| $R_s$ | Radius of the stator | 28 | mm |
| $R_r$ | Radius of the rotor | 27 | mm |
| $R_w$ | Distance of the winding from rotor axis | 30 | mm |
| $R_f$ | Radius to the Shaft | 7.5 | mm |
| $R_d$ | Radius of shaft hole in the frame | 8 | mm |
| $W_d$ | Width of the slot opening | 3 | mm |
| $W_l$ | Width of the coil from coil side | 6.5 | mm |
| $W_h$ | Height of the coil that lay on coil side | 12 | mm |
| $W_g$ | Gap between adjacent coil | 0.12 | mm |
| $W_{in}$ | Insulation thickness | 1 | mm |
| h | Height of the coil | 12 | mm |
| $L_{stk}$ | Stack length | 52.6 | mm |
| $L_e$ | Length of rotor that face to the end winding | 5 | mm |
| $L_w$ | Width of the bearing guard in the frame | 5 | mm |
| $r_b$ | Radius of the ball of bearing | 2.975 | mm |
| $r_c$ | Radius of clearance with ball | 2.985 | mm |
| $N_b$ | No. of balls in the bearing (6202z/ 6201z) | 8/ 7 | |
| $\varepsilon_{lb}$ | R. permittivity of lubricant | 2 | |
| $\varepsilon_{in}$ | R. permittivity of the insulation | 3 | |
| $\varepsilon_0$ | Permittivity of the air | - | |
| $S$ | No. of slots or coil sides | 9 | |

### B. Calculation of all parasitic capacitances

Based on the geometry of the motor, all parasitic capacitances of the PMSM are determined, as shown in Fig. 2 (a). Each parasitic capacitance can be calculated as follows

$$Csw = \frac{\frac{S}{3}\varepsilon_0\varepsilon_{in}2(W_h+W_l)L_{stk}}{W_{in}} \tag{1}$$

$$Crw = \frac{\frac{S}{3}\varepsilon_0 W_d L_{stk}}{R_w - R_r} + \frac{4\pi\varepsilon_0 L_e}{3\ln\frac{R_s+R_w}{2R_r}} \tag{2}$$

$$Csr = \frac{2\pi\varepsilon_0 L_{stk}}{\ln\frac{R_s}{R_r}} \tag{3}$$

$$Csh = \frac{4\pi\varepsilon_0 L_w}{\ln\frac{R_d}{R_f}} \tag{4}$$

$$Cww = \frac{\frac{S}{3}\varepsilon_0 h L_{stk}}{W_g} \tag{5}$$

$$Cb = \frac{N_b\pi\varepsilon_0\varepsilon_{lb}L_b}{3\ln\left(\frac{r_c}{r_b}\right)};\ L_b = r_c/2 \tag{6}$$

### C. Equivalent circuit by all parasitic capacitances

Fig. 3 shows the equivalent circuit of parasitic capacitance. The three-phase windings are connected to current sensor controlled by SVPWM. Using the equivalent circuit, all parasitic capacitances can be obtained. In addition, Vsh can be calculated using stator-to-rotor, end bearing, and rotor-to-winding capacitances as (7).

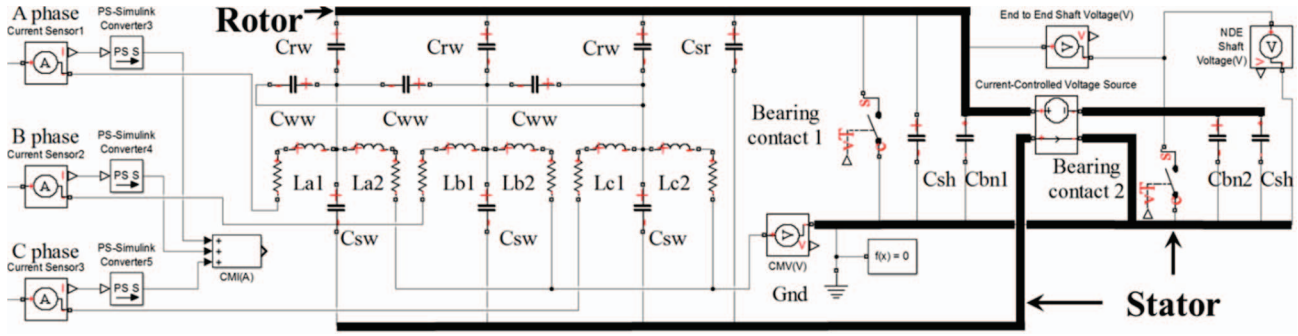


Fig. 3. Equivalent circuit by parasitic capacitances.

$$V_{sh} = \frac{CMV}{\frac{Csr + Cbt}{3Crw} + 1}; \quad CMV = \frac{V_{a,gnd} + V_{b,gnd} + V_{c,gnd}}{3} \tag{7}$$

## III. Motor Design due to Variation of All Parasitic Capacitances for Mitigation of the Shaft Voltage

Several parasitic capacitances exist in the motor due to the geometry of the motor. In addition, the shaft voltage can be reduced by changing of the parasitic capacitances. Based on the equivalent circuit, we propose the mitigation method by changing the values of parasitic capacitances. Some of them affect the shaft voltage, not all. Thus, it needs to distinguish the parasitic capacitances that affect the shaft voltage. First, we analyzed characteristics and the effect of each parasitic capacitance to determine which capacitances affect the shaft voltage. Then, we propose three types of models according to change in the value of the parasitic capacitances.

### *A. Characteristics and effects of each parasitic capacitance*

Csw is the capacitance occurred between the stator and the winding. The value of the Csw depends on the thickness of the insulator of coil side. For this reason, leakage flux of the coil side is increased as the increasing of the insulator thickness. However, it does not affect the Vsh.

Csr is the capacitance occurred by the distance between the stator and the rotor. Thus, it depends on an air-gap length. Specifically, shaft voltage can be reduced by increase in the Csr. For this reason, increase in the Csr causes decrease in the air-gap, so that it increases the motor performance.

Cb is the ball bearing capacitance, which is a critical component for the shaft voltage. In this study, the test motor uses two types of ball bearings such as 6201Z (drive end side) and 6202Z (non-drive end side). Practically, Cb cannot be changed because standard of industrial bearings is fixed according to size, so that Cb also didn't consider as a parameter for reducing the shaft voltage.

Crw is the capacitance occurred by the distance between the rotor and the winding. It is the most problematic capacitance for the shaft voltage schema because the CMV of the winding transfers to the rotor through the Crw. Although the distance between the rotor and the winding includes an air-gap length, Crw can be changed with constant air-gap length by changing the winding configuration.

### *B. Different models according to parasitic capacitances*

Different models according to parasitic capacitance types are proposed and analyzed in order to determine the appropriate models for reducing the shaft voltage, as shown in Figs. 4, 5, and 6. Specifically, each model is designed by changing the winding shape considering the insulator thickness, number of winding turns, and fill factor. First, Fig. 4 shows the four types models according to change in the Csw. The distance between the stator and the winding was changed by increasing the insulator thickness. Fig. 5 shows the four types models according to change in the Csr. Here, the air-gap length is changed with the maintenance of the inner diameter of the stator. Fig. 6 shows the different types of models according to change in the Crw. Here, winding shape is modified to change the Crw values without changes in the air-gap length. As a result, the Csw does not affect the shaft voltage, as shown in Table III. On the other hand, we confirmed that the variation of the Csr and the Crw affect the shaft voltage, as shown in Tables IV and V.

## IV. Results and Discussion

Fig. 7 shows the variation of the $V_{sh}$ according to change in the Csw, Csr, and Crw. Here, we confirmed that Csw is not related to the $V_{sh}$ because $V_{sh}$ maintains constant value although the Csw is changed, as shown in Fig. 7 (a). On the other hand, $V_{sh}$ is decreased as the increase in the Csr and increased as the increase in the Crw, as shown in Figs. 7 (b) and (c). In case of the Csr, it causes reduction of the average torque ($T_{avg}$), as shown in Fig. 8 (b). Thus, Csr is not appropriate parasitic capacitance to reduce the shaft voltage. However, $T_{avg}$ maintains constant value according to change in the Crw, as shown in Fig. 8 (c). Therefore, decreasing the Crw is appropriate method to decrease the $V_{sh}$ although it causes the increase in the torque ripple ($T_{ripple}$).

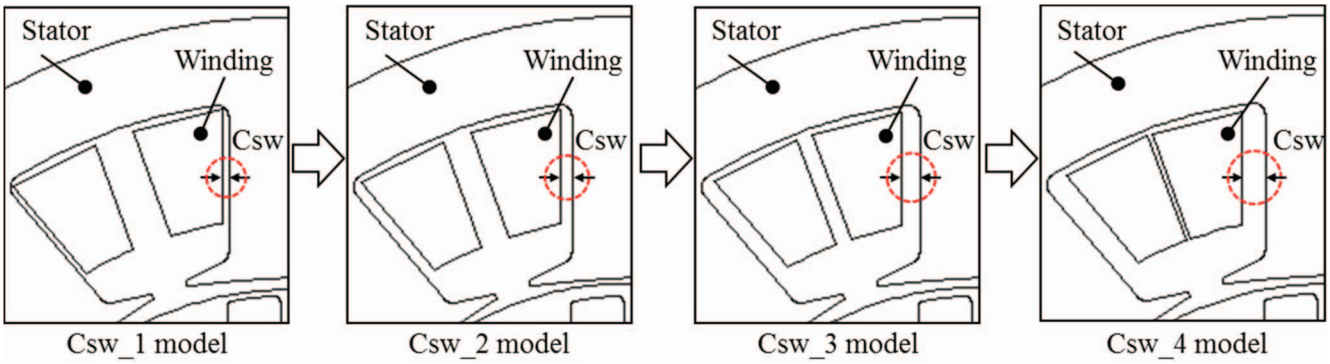


Fig. 4. Different type of models according to change in Csw.

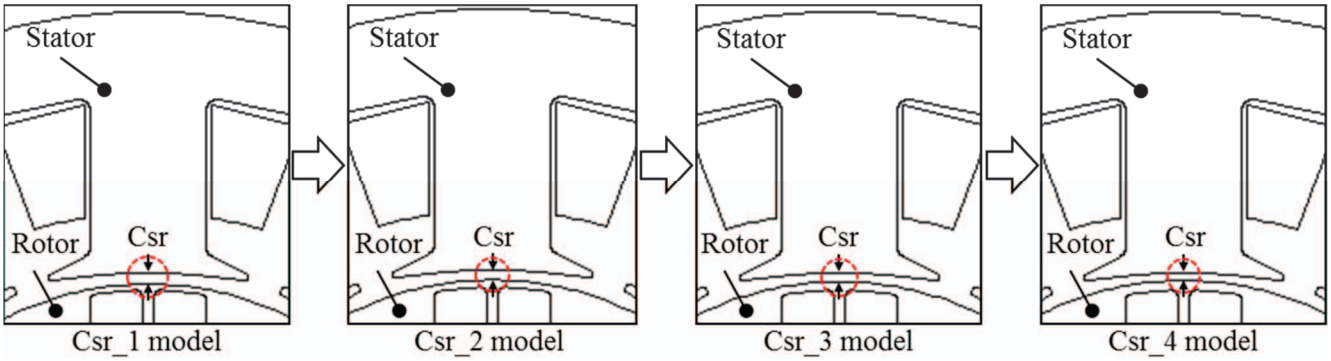


Fig. 5. Different type of models according to change in Csr.

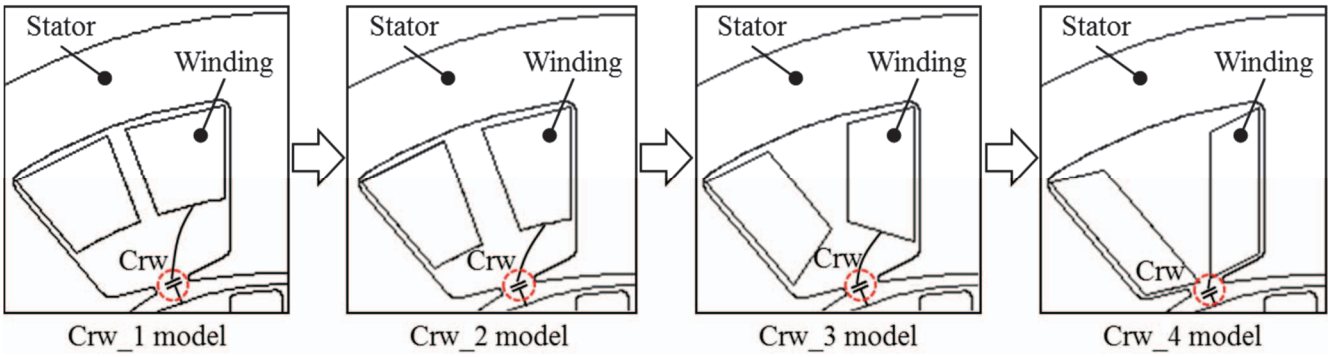


Fig. 6. Different type of models according to change in Crw.

TABLE III:
The dimensions of the motor according to variation of the Csw

**$\varepsilon_0$: 8.8419e-12, $\varepsilon_{in}$: 3**

| Item | $R_r$ (mm) | $R_r$ (mm) | $R_w$ (mm) | $W_d$ (mm) | $W_g$ (mm) | $W_h$ (mm) | $W_l$ (mm) | $W_{in}$ (mm) | H (mm) | $L_{stk}$ (mm) | $L_e$ (mm) | S |
|---|---|---|---|---|---|---|---|---|---|---|---|---|
| Csw_1 | 28 | 27 | 32.7 | 3 | 2.4 | 12 | 6.5 | 0.5 | 8.28 | 52.6 | 6 | 9 |
| Csw_2 | 28 | 27 | 32.7 | 3 | 4.3 | 12 | 6.5 | 1.0 | 9.77 | 52.6 | 6 | 9 |
| Csw_3 | 28 | 27 | 32.7 | 3 | 4.3 | 12 | 6.5 | 1.5 | 10.87 | 52.6 | 6 | 9 |
| Csw_4 | 28 | 27 | 32.7 | 3 | 3.3 | 12 | 6.5 | 2.0 | 13.16 | 52.6 | 6 | 9 |

TABLE IV:
The dimensions of the motor according to variation of the Csr

| Item | $R_s$ (mm) | $R_r$ (mm) | $R_w$ (mm) | $W_d$ (mm) | $W_g$ (mm) | $W_h$ (mm) | $W_l$ (mm) | $W_{in}$ (mm) | H (mm) | $L_{stk}$ (mm) | $L_e$ (mm) | S |
|---|---|---|---|---|---|---|---|---|---|---|---|---|
| Csr_1 | 28 | 27 | 32.7 | 3 | 2.4 | 12 | 6.5 | 0.5 | 8.28 | 52.6 | 6 | 9 |
| Csr_2 | 28 | 27.1 | 32.7 | 3 | 4.3 | 12 | 6.5 | 0.5 | 9.77 | 52.6 | 6 | 9 |
| Csr_3 | 28 | 27.2 | 32.7 | 3 | 4.3 | 12 | 6.5 | 0.5 | 10.87 | 52.6 | 6 | 9 |
| Csr_4 | 28 | 27.3 | 32.7 | 3 | 3.3 | 12 | 6.5 | 0.5 | 13.16 | 52.6 | 6 | 9 |

TABLE V:
The dimensions of the motor according to variation of the Crw

| Item | $R_s$ (mm) | $R_r$ (mm) | $R_w$ (mm) | $W_d$ (mm) | $W_g$ (mm) | $W_h$ (mm) | $W_l$ (mm) | $W_{in}$ (mm) | H (mm) | $L_{stk}$ (mm) | $L_e$ (mm) | S |
|---|---|---|---|---|---|---|---|---|---|---|---|---|
| Crw_1 | 28 | 27 | 34.2 | 3 | 2.4 | 7.79 | 8.93 | 0.5 | 8.28 | 52.6 | 6 | 9 |
| Crw_2 | 28 | 27 | 32.7 | 3 | 4.3 | 9.3 | 7.19 | 0.5 | 9.77 | 52.6 | 6 | 9 |
| Crw_3 | 28 | 27 | 31.6 | 3 | 4.3 | 10.39 | 7.19 | 0.5 | 10.87 | 52.6 | 6 | 9 |
| Crw_4 | 28 | 27 | 29.3 | 3 | 3.3 | 11.91 | 4.65 | 0.5 | 13.16 | 52.6 | 6 | 9 |

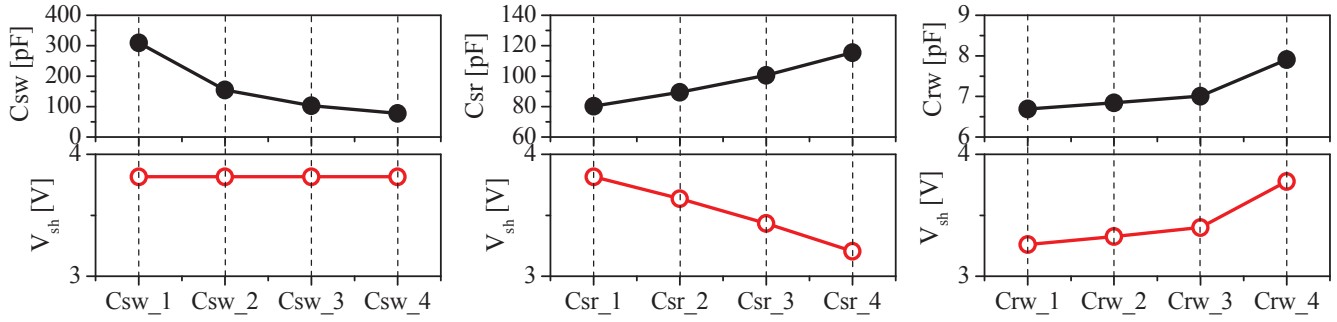


Fig. 7. Variation of the $V_{sh}$ according to variation of Csw, Csr, and Crw. (a) $V_{sh}$ according to Csw. (b) $V_{sh}$ according to Csr. (c) $V_{sh}$ according to Crw.

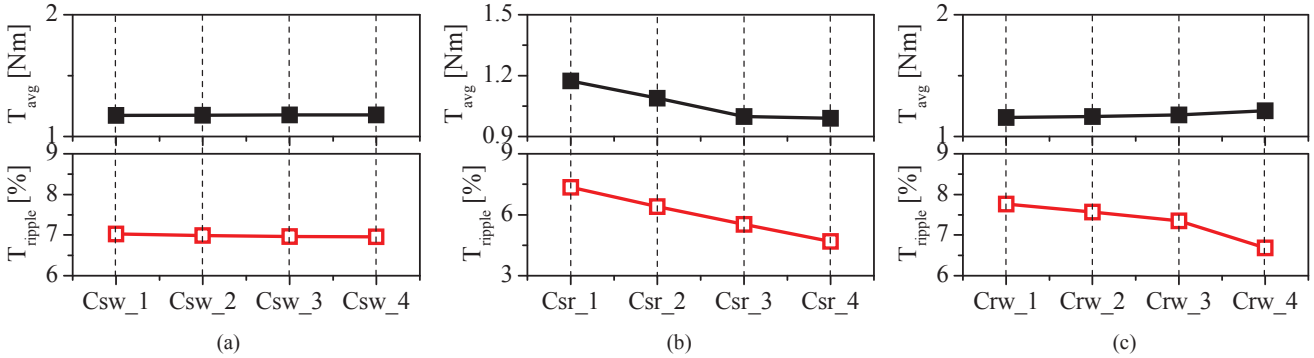


Fig. 8. Variation of the $T_{avg}$ and $T_{ripple}$ according to variation of Csw, Csr, and Crw. (a) $T_{avg}$ and $T_{ripple}$ according to Csw.(b) $T_{avg}$ and $T_{ripple}$ according to Csr.(c) $T_{avg}$ and $T_{ripple}$ according to Crw.

## V. Conclusion

This paper proposes the mitigation method of the shaft voltage according to change in parasitic capacitances. First, equivalent circuit made by all parasitic capacitances is introduced. Then, shaft voltage and output torque characteristics are respectively analyzed by introduced equivalent circuit and finite element method simulation tool, ANSYS MAXWELL. Finally, we confirmed that variation of the Csw does not affect both the shaft voltage and the torque characteristics. On the other hand, Crw and Csr affect the shaft voltage and the torque characteristics. However, influence of the Crw on the torque characteristics is very insignificant, compared with that of Csr. Thus, Crw is determined as an appropriate parasitic capacitance for reducing the shaft voltage by changing the winding shape.

## Acknowledgement

This work was supported by Industrial Strategic Technology Development Program of Korea Evaluation Institute of Industrial Technology (KEIT) (No. 10062426) and the Technology Innovation Program (No. 10043799, Development of environment-friendly 200kW electric propulsion module and SW based control technology for small ship) funded By the Ministry of Trade, industry & Energy (MI, Korea).

## Reference

[1] S. S. Kwak and S. K. Mun, “Model predictive control methods to reduce common-mode voltage for three-phase voltage source inverters,” *IEEE Trans. Power Electron*., vol. 30, no. 9, pp. 5019-5035, Sep. 2015.

[2] T, Maetani, S. Morimoto, K. Yamamoto, Y. Isomura, and A. Watanabe, “Comparing brushless DC motors: A method of suppressing the shaft voltage even in a grounded motor frame,” *IEEE Ind. Appl. Magazine*, vol. 21, no. , pp. 29–35, Nov./Dec. 2015.

[3] J. Adabi, F. Zare, A. Ghosh, and R. D. Lorenz, “Calculations of capacitive coupling in induction generators to analyse shaft voltage,” *IEEE Trans. IET Power Electron*., vol. 3, no. 3, pp. 379-390, 2010.

[4] S. Chen, T. A. Lipo and D. Fitzgerald, "Modeling of motor bearing currents in PWM inverter drives," *IEEE Trans. Ind. Appl.*, vol. 32, no. 6, pp. 1365–1370, Nov./Dec.1996.

[5] S. Chen, T. A. Lipo and D. Fitzgerald, “Source of induction motor bearing currents caused by PWM inverters” *IEEE Trans. Energy Conversion*, vol. 11, no.1, Mar. 1996.

[6] D. Busse, J. Erdman, R. J. Kerkman, D. Schlegel, and G. Skibinski, "System electrical parameters and their effects on bearing currents," *IEEE Trans. Ind. Appl*., vol. 33, no. 2, pp. 577-584, Mar./Apr. 1997.

[7] U. T. Shami and H. Akagi “Identification and discussion of the origin of a shaft end-to-end voltage in an inverter-driven motor” *IEEE Trans. Power Electron.,* vol. 25, no. 6, Jun. 2010.

[8] A. Muetze, and A. Binder “Calculation of circulating bearing currents in machines of inverter-based drive systems” *IEEE Trans. Ind. Electron*., vol. 54, no. 2, Apr. 2007.